

EARTHQUAKE OBSERVATIONS AND ANALYSIS
OF LNG TANK ON PILE FOUNDATION

by

Katuyuki Dewa^I, Michitaka Hirose^{II}, Ichiro Saito^I and Akira Ohira^I

SUMMARY

A tank constructed on soft ground shows complex behavior in an earthquake. In order to investigate the dynamic properties of soil and tank, earthquake observations were made on LNG tanks. Analysis of records from the observations have yielded useful information. Based on the information, two tanks were represented as multi-mass systems considering the interaction between the tanks. The computed responses of the systems agreed well with the observed records. Furthermore, the behaviors of soil and tank during strong motions were inferred from non-linear analyses in which the soil had hysteresis characteristics of the Hardin-Drnevich type.

EARTHQUAKE OBSERVATIONS

Outline. Earthquake observations were carried out on two 75,000 KL LNG tanks. Fig. 1 shows the profiles of the soil and tank. The surface layer consisted of the following three formations: fill, alluvial silt and diluvial sand. The base layer was stiff solidified silt. Both tanks were cylindrical in shape having identical diameters of 59.4 m and heights of 42.9m. The distance between their centers was 66 m. The tank bases were of double-slab type each supported on 691 steel piles driven to about GL -23 m. Accelerometers were set at three points on each tank base and five points on each tank top, and in order to measure ground behavior, at the two levels of GL -1 m and GL -30 m, as shown in Fig. 2. Four earthquakes have been recorded since March 1977. Their maximum accelerations ranged from 3.8 to 11.2 gal at the surface.

Results. The distributions of amplifications are shown in Fig. 3 in which the average of maximum accelerations recorded at various points are normalized by the average of the horizontal components at GL -30 m. It was found that amplification at the tank base was less than at the surface, and that the relatively small difference between amplifications at the tank top and at the tank base was indicative of the little rocking of the tank.

The solid line in Fig. 4 shows the average transfer function (GL -1 m / GL -30 m) computed from all data. It approximately represents the frequency characteristics of the surface layer. The natural periods of the soil were found to be 0.53 sec for the first and 0.19 sec for the second. The natural periods and participation factors of the multi-mass systems representing the soil formation were computed for the sake of assuming damping constants. The natural periods computed were quite similar to those observed, and so

-
- I. Civil Design Department, Shimizu Construction Co., Ltd.
II. The Research Laboratory of Shimizu Construction Co., Ltd.

making use of Eq. 1, the damping constants of the soil were assumed as follows: 8% for the first mode and 5% for the second.

$$h_i = \beta_i / (2 \cdot \pi) \quad \dots\dots\dots \text{Eq. 1}$$

where h_i , β_i and π represent damping constant, participation factor and amplification in the transfer function for the i -th mode, respectively. The dotted line in Fig. 4 shows the transfer function of the system for the assumed damping constants. The average transfer function (Tank Base / GL -30 m) is shown as Fig. 5. The natural periods of the tank foundation alone were 0.42 sec for the first mode and 0.19 sec for the second. In the same manner for soil, it was assumed that damping constants were 9% for the first mode and 8% for the second.

NUMERICAL ANALYSES BY MULTI-MASS SYSTEMS

Simulation Analysis. Fig. 6 shows the analytical model in which the soil, the two tanks, and the soil between the two tanks were represented as multi-mass systems. LNG in a tank would shake separately from the tank foundation and soil because of considerably different natural periods. Therefore, only the weight of LNG was added to the tank and the tank base, and sloshing of the LNG was neglected. The interaction of the two tanks was estimated by means of connecting the model which represented the soil between the two tanks through interaction springs. The stiffnesses of interaction springs were evaluated by multiplying the stiffness of a pile derived by Mindrin's Second Solution by 29 (the number of piles arrayed on the center line of the tank base). The acceleration recorded at GL -30 m in the Izu Oshima Kinkai Earthquake of 1978 was adopted as the ground motion in the analysis. The damping matrices were constructed as Caughey's series¹ based upon the damping constants assumed above.

Fig. 7 shows the distributions of maximum acceleration responses. Owing to the difference in the liquid levels (Tank A: 6.6 m, Tank B: 27.4 m), the maximum acceleration of Tank B exceeded that of Tank A. Acceleration responses are shown in Fig. 8 in comparison with observed records. It was found that the interactive tank-soil systems could simulate actual dynamic behaviors of tanks and soil very well.

Non-linear Analysis. It is generally known that the shear modulus of soil decreases with increase in the strain developed. In order to investigate the behaviors of soil and a tank under strong motions, analysis were carried out for the ground motion of the record observed El Centro (1940), the maximum acceleration of which was modified to 150 gal. In the analysis, the soil had hysteresis characteristics of the Hardin-Drnevich type²), but the tank foundation and the interaction springs were still linear. Fig. 9 shows the distributions of the maximum responses. It was found that the acceleration decreased in fill owing to considerable decrease in the shear modulus. As for moments of piles, it was interesting since large moments were developed not only at pile-heads, but also boundaries between alluvial silt and diluvial sand because of the difference in stiffnesses.

REFERENCES

- 1) T.K. Caughey: "Classical Normal Modes in Damped Linear Dynamic Systems," Jour. of Appl. Mech., Sept. 1964.
- 2) B.O. Hardin and V.P. Drnevich: "Shear Modulus and Damping in Soils: Design Equation and Curves," ASCE, SM7, July 1972.

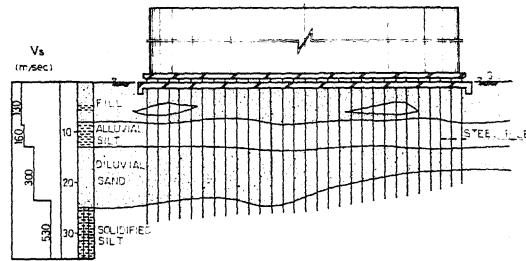


Fig. 1 Profiles of Soil and Tank.

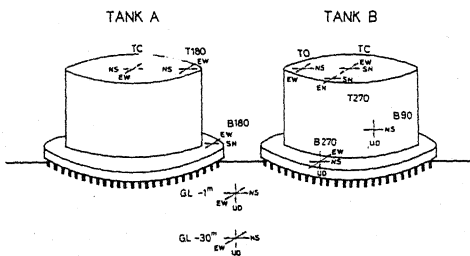


Fig. 2 Display of Accelerometers

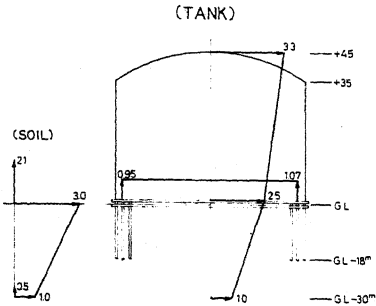


Fig. 3 Distributions of Amplifications

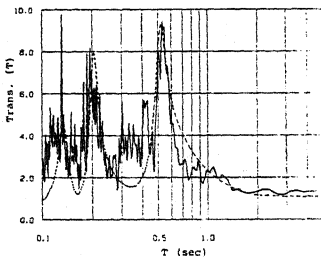


Fig. 4 Average Transfer Function
(GL -1 m / GL -30 m)

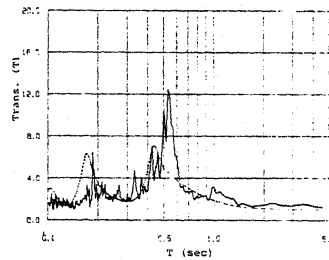


Fig. 5 Average Transfer Function
(Tank Base / GL -30 m)

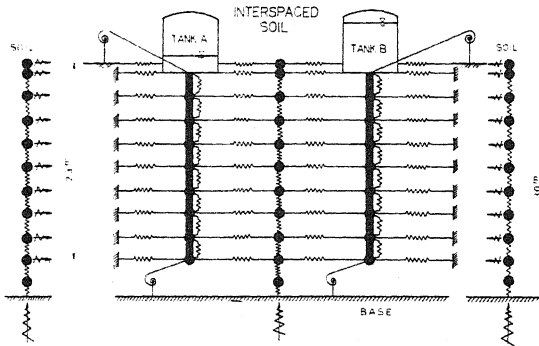


Fig. 6 Analytical Model

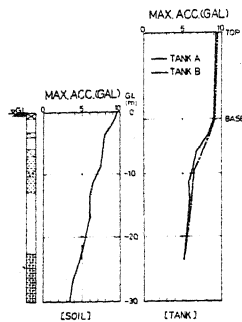


Fig. 7 Distributions of Maximum Response

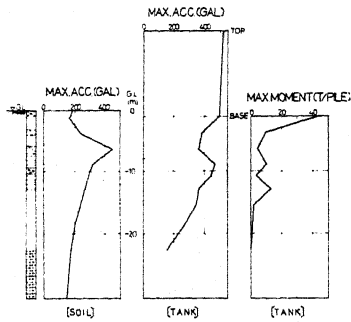


Fig. 9 Distributions of Maximum Response

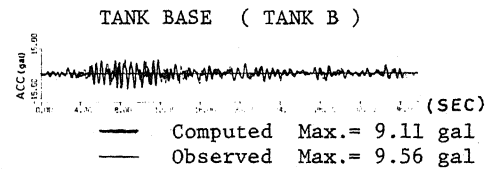
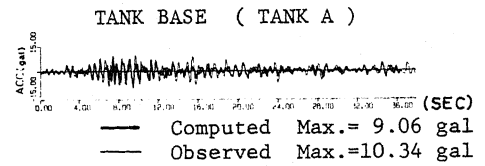
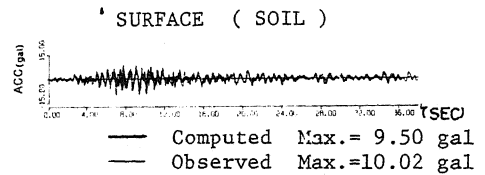


Fig. 8 Acceleration Responses